water

MDPI

Article

Stable Isotope Monitoring in a Semi-Arid Olive Orchard Suggest Changes in Ecohydrological Dynamics from Contrasting Drip Irrigation Regimes

Taha Attou [1,2,*], M. H. Kharrou [1], S. Kuppel [2], Y. Ait Brahim [1], L. Bouchaou [1,3], V. Demarez [4], M. M. Lehmann [5], F. Raibi [1,6], T. Elghali [6], A. Elazhari [1,7], N. Rhoujjati [8], H. Bouimouass [9] and A. Chehbouni [9]

1 International Water Research Institute, Mohammed VI Polytechnic University, Benguerir 43150, Morocco; mohamed.kharrou@um6p.ma (M.H.K.); yassine.aitbrahim@um6p.ma (Y.A.B.); lhoussaine.bouchaou@um6p.ma (L.B.); fatima.raibi@um6p.ma (F.R.); ahmed.elazhari@um6p.ma (A.E.)
2 Géosciences Environnement Toulouse, Université de Toulouse/CNRS/IRD/CNES, 31400 Toulouse, France; sylvain.kuppel@ird.fr
3 Laboratory of Applied Geology and Geo-Environment, Faculty of Science, Ibn Zohr University, Agadir 80000, Morocco
4 Université de Toulouse, CNRS, CNES, INRAe, IRD, CESBIO, Centre d'Etudes Spatiales de la Biosphère, 31400 Toulouse, France; valerie.demarez@utoulouse.fr
5 Forest and Soil Ecology, Swiss Federal Institute for Forest, Snow and Landscape Research WSL, Zürcherstrasse 111, 8903 Birmensdorf, Switzerland; marco.lehmann@wsl.ch
6 Centre National de l'Énergie, des Sciences et des Techniques Nucléaires (CNESTEN), Rabat 14000, Morocco; elghali.tibari@gmail.com
7 Geotop-UQAM, Hydro Sciences, Department of Earth and Atmospheric Sciences, University of Quebec at Montreal (UQAM), Montreal, QC H3C 3P8, Canada
8 Geoenvironment and Civil Engineering (L3G), Laboratory of Georessources, Faculty of Science and Technology, Cadi Ayyad University (UCA), Av. A. El Khattabi, Marrakech 40000, Morocco; nadiarhoujjati@gmail.com
9 Center for Remote Sensing Applications, Mohammed VI Polytechnic University, Benguerir 43150, Morocco; houssne.bouimouass@um6p.ma (H.B.); abdelghani.chehbouni@um6p.ma (A.C.)
* Correspondence: taha.attou@um6p.ma or taha.attou.th@gmail.com; Tel.: +212-661809887

check for updates

Academic Editors: Carmen Maftei and Ashok Vaseashta

Received: 30 July 2025
Revised: 20 August 2025
Accepted: 27 August 2025
Published: 22 October 2025

Citation: Attou, T.; Kharrou, M.H.; Kuppel, S.; Ait Brahim, Y.; Bouchaou, L.; Demarez, V.; Lehmann, M.M.; Raibi, F.; Elghali, T.; Elazhari, A.; et al. Stable Isotope Monitoring in a Semi-Arid Olive Orchard Suggest Changes in Ecohydrological Dynamics from Contrasting Drip Irrigation Regimes. *Water* **2025**, *17*, 3029. https://doi.org/10.3390/w17213029

Copyright: © 2025 by the authors. Licensee MDPI, Basel, Switzerland. This article is an open access article distributed under the terms and conditions of the Creative Commons Attribution (CC BY) license (https://creativecommons.org/licenses/by/4.0/).

Abstract

In semi-arid regions of Morocco, where the majority of water withdrawals are devoted to irrigation, optimizing irrigation practices in agriculture is a national priority in the face of recurring droughts and growing pressure on groundwater resources. However, the hydrological impacts of different drip-irrigation systems in the soil–plant–atmosphere continuum remain insufficiently understood. We monitored the stable isotope composition (δ^2H, $\delta^{18}O$) across the two agricultural plots in Marrakech (Morocco) with surface drip and subsurface drip irrigation treatments for a complete hydrologic year (June 2022 to June 2023). Weekly to daily samples of rainfall, irrigation water, groundwater, and soil at various depths (5–50 cm) were sampled, and water from branch xylem was extracted using the cryogenic vacuum distillation method. We found that the subsurface irrigation treatment, which delivered water directly to the root zone, maintained narrow isotopic ranges in water of soils beyond 30 cm, as well as in branch xylem and leaf water. By contrast, surface irrigation treatment plots showed pronounced evaporative isotopic enrichment: summer topsoil water $\delta^{18}O$ peaked at −1.1‰ (vs. −8.7‰ in subsurface irrigation treatment), and leaf water reached +13‰ (vs. +8‰ in subsurface). Despite this larger isotopic heterogeneity in surface irrigation site, branch xylem water $\delta^{18}O$ remained within −6 to 2.5‰ across all soil depth, similar to subsurface irrigation treatment, which ranged between −5 and 0‰. This suggests that olive roots accessed soil water uniformly from the upper 50 cm under both irrigation treatments. Seasonal xylem isotopic enrichment in spring and midsummer mirrored shifts towards shallow, evaporatively altered soil water under surface irrigation, but not under the subsurface. The results suggest that subsurface drip irrigation can significantly improve

drought resilience and water-use efficiency in the expanding olive sector of the Maghreb, while continuous isotope monitoring serves as a practical approach to enhance sustainable and adaptive water management in water-limited regions.

Keywords: soil–plant–atmosphere continuum (SPAC); irrigation management; stable isotopes of water; isotope hydrology; cryogenic vacuum distillation

1. Introduction

Water is a critical resource for agriculture, industry, and the environment, particularly in semi-arid and arid regions where increasing water scarcity poses serious challenges [1]. Factors such as population growth, agricultural intensification, and climate change have intensified stress on freshwater supplies, making it difficult to balance water allocations among competing sectors [2]. In agriculture, specifically, a consistent water supply is crucial for maintaining robust crop yields and ensuring global food security [3]. However, due to the changing climate, weather patterns have become more erratic, characterized by a higher frequency of extreme events especially droughts, caused by higher temperature and reduced rainfall in semi-arid regions [4], where a significant share of the irrigation expansion is precisely taking place [5]. This situation underscores the necessity of understanding the dynamics of water and its movement through soil, absorption by crops, and subsequent evaporation into the atmosphere. Mastering this concept is crucial for ensuring efficient water usage in agriculture in areas that are currently experiencing significant water scarcity [6].

In semi-arid regions like Morocco, improving irrigation efficiency is crucial for sustainable agriculture [7]. Traditionally, flood irrigation has been the most common method, where this technique results in high water losses due to evaporation and deep percolation, making it unsuitable for water-scarce regions [8]. Recognizing the need for a more sustainable approach, the Moroccan government launched the Green Morocco Plan in 2008, a comprehensive agricultural strategy aimed at modernizing farming practices and optimizing water resources, followed by the Green Generation plan in 2020. A key initiative within this framework was the National Irrigation Water Saving Program (PNEEI), which set an ambitious goal of converting from flood irrigation to localized irrigation systems, particularly drip irrigation. By reducing water losses and increasing crop productivity, the plan played a transformative role in Morocco's agricultural landscape.

As a result, many studies have compared irrigation systems in Morocco in terms of water savings and irrigation efficiency. For instance, a recent study [9] demonstrated that seasonal deep percolation losses under flood irrigation reached up to 53% of total water input, with an associated irrigation recharge efficiency of only 44%, compared to 21% losses and up to 78% efficiency under drip irrigation in olive orchards of the Haouz Plain.

However, while conventional water balance approaches are useful for estimating gross irrigation performance, they often lack the resolution to track how water is distributed and used within the root zone and beyond [10]. This is particularly relevant when comparing irrigation strategies such as surface versus subsurface drip irrigation, where water delivery depth may alter plant uptake patterns and soil moisture retention in subtle ways. In this context, stable isotopes of hydrogen (δ^2H) and oxygen ($\delta^{18}O$) have become valuable tools for investigating water fluxes within the soil–plant atmosphere continuum (SPAC) [11,12]. By analyzing the isotopic composition of water at different points in the SPAC such as in the soil profile, plant xylem, and atmospheric vapor, researchers can trace the origins and pathways of water with a level of detail not easily achievable by other methods [13,14]. This

approach facilitates the assessment of key processes, including evapotranspiration, soil moisture distribution, and deep percolation. Global studies leveraging these techniques have shown their effectiveness in diverse agro-ecological settings, including semi-arid regions of Morocco, where efficient irrigation strategies are urgently needed to conserve limited water resources [15]. At the same time, the successful application of isotopic methods depends on robust sampling protocols and reliable extraction methods that minimize artifacts such as evaporation fractionation and sample contamination, while also accounting for the inherent limitations and biases introduced by laboratory constraints [16].

For instance, the stable isotope method provides a promising tool for partitioning evapotranspiration (ET). This method has been successfully used in many studies related to water movement in the soil–vegetation–atmosphere continuum [17–19] since the measurements of stable isotopic compositions are now relatively easy and robust due to the rapid progress in development of mass and laser spectrometry devices during the last few years. Water uptake by plants was treated as essentially non-fractionating, so the isotope ratio that moves from soil through roots, stems, and into the xylem is assumed to match that of the source water [20]. More recent studies nonetheless show that minor isotopic offsets can occur along the soil–root–stem–leaf continuum. But these deviations are an order of magnitude smaller than the enrichment produced by direct evaporation and are therefore often neglected in practice [21]. By contrast, water evaporated from soil surfaces is strongly fractionated and depleted in heavy isotopes [22]. This "isotopic fingerprinting" may also help to understand groundwater recharge and dynamics in arid environments [23], including the impact or agricultural practices [24]. For example, Aouade et al. [15] combined δ^2H measurements of soil water, xylem sap, and canopy-layer vapor with concurrent eddy covariance fluxes over an irrigated winter wheat field near Marrakech. Their SPAC-based mass balance showed that transpiration dominated post-irrigation water losses (about 70% of total ET) and rose to nearly 80% under drier pre-irrigated soil, translating to roughly 4–5 mm d^{-1} of plant water use versus 1–2 mm d^{-1} of soil evaporation. This field scale demonstration confirms that integrating isotopic profiles with micrometeorological data can allow partitioning ET into both soil evaporation and plant transpiration, offering a pathway for improving irrigation scheduling in semi-arid agriculture.

Therefore, the present study examines the hydrological performance of two irrigation systems: surface drip irrigation (DI) and subsurface drip irrigation (SDI) in a semi-arid agricultural setting. Specifically, it compares their water fluxes within the SPAC through an isotopic analysis. Such an integrative strategy reveals not only the overall water balance but also the spatial and temporal nuances of water uptake by plants, including the depth at which roots predominantly acquire water under varying irrigation practices. In this study we aim to add information on the gap and interconnect between these previous studies conducted in the Moroccan context. The central hypotheses of this work are the following:

1. Isotopic range of the soil profile is narrower in SDI than in DI, depending on the seasonal cycle in the isotopic composition of rainwater?
2. Soil and plant water experience more evaporative, non-productive loss of water under DI than under SDI, as indicated by the isotopic enrichment in topsoil.
3. Plants under SDI take consistently water from the subsurface irrigation layer throughout the season, while under DI it takes mainly water from the topsoil.

By testing these hypotheses through a careful synthesis of isotopic data, this study seeks to elucidate the complex interactions among soil, plant, and atmospheric components under contrasting irrigation regimes. The finding of DI will help refine our understanding of water partitioning in agricultural systems, informing the development of water-saving strategies, improving irrigation scheduling, and ultimately contributing to more sustainable management of scarce water resources in regions facing escalating climatic and hydrological pressures.

2. Materials and Methods

2.1. Study Area

The study was conducted in a semi-arid olive orchard located near Marrakech, called Agdal Domain, where planted with 240-year-old olive trees, grown in an orchard of about 275 ha. The density of olive trees was about 225 trees per hectare, which corresponds to an area of about 45 m^2 occupied by each tree. The area, (Latitude 31.587491 | Longitude: −7.980781 | 489 m elevation) is characterized by flat terrain, warm temperatures, and notably scarce and erratic rainfall. The average annual temperature in this region ranges from 12 °C in winter to 30 °C in summer, with occasional peaks exceeding 40 °C during heatwaves. Rainfall in Marrakech is typically between 200 mm and 250 mm per year, occurring mainly in the winter months, with long dry periods during the summer. These conditions contribute to the region's semi-arid climate. This region's climate is further marked by moderate to strong winds, with average wind speeds ranging from 15 to 30 km/h, and high evapotranspiration rates reaching up to 1600 mm per year, depending on seasonal variations in hot and windy conditions [25]. The orchard's soils, composed of roughly 30% clay, 44% sand, and 25% silt, reflect a texture that can retain a reasonable amount of water (field capacity of about 32%) but is still vulnerable to drying (wilting point around 19%), particularly under the hot and windy conditions [26]. These soil properties were determined using the pedotransfer function described by Wösten et al. [27], providing valuable insights into how the orchard's soil stores and releases water across seasons. The water table in the region varies, but in general, groundwater is found at depths of 30 to 260 m, depending on the proximity to natural water sources. The depth of the groundwater table and its recharge rates vary seasonally, influenced by a complex interplay between natural precipitation patterns, the demands of agricultural water use, and the impact of various on-farm practices. For instance, natural rainfall contributes significantly to the replenishment of groundwater, though its spatially and temporally heterogeneous distribution makes it difficult to rely on as a sole source of recharge. Agricultural water use also plays a key role, particularly during peak irrigation periods when the demand for water increases. On-farm practices, such as fertilization, tillage, and crop rotation, further influence the efficiency of water usage and the sustainability of water resources [28].

Water for irrigation in the studied olive orchard is primarily sourced from wells, with additional reserves provided by nearby dams and seguias, creating a dual water supply system that is essential for coping with the region's fluctuating and heterogenous rainfall patterns. This combined use of different water sources is common and reflects regional efforts to adapt to the uncertainties of semi-arid climates and ensure a consistent and reliable water supply for agricultural purposes. Two irrigation systems: surface drip (DI) and subsurface drip (SDI) are used to optimize water-use efficiency for olive production under challenging climate conditions (Figure 1). In the surface drip irrigation system, pierced plastic lines deliver water to the soil surface near the base of each tree. In contrast, in the subsurface system the drip lines are buried at 30 cm depth, therefore supplying water closer to the root system, aiming at reducing direct evaporation and improving moisture retention (especially during dry spells). Both the surface (DI) and subsurface (SDI) drip irrigation systems were equipped with self-compensating drippers, each delivering an average flow rate of 2.3 L h^{-1} under a pressure of 1 bar. These systems represent both classical and improved drip irrigation methods, allowing local farmers to adapt to water scarcity. The choice between surface and subsurface drip systems is influenced by soil type and water availability. Subsurface drippers, effectively conserve water and deliver moisture to the root zone. The sampling stations were distributed over various emitter distances, soil profiles, and phenological stages to represent the spatial and temporal variability of the orchard (see Section 2.2). This approach embodies daily orchard management, when

farmers continuously adjust practices in response to fluctuating weather, crop demand, and water availability. These elements create a dynamic environment for evaluating water fluxes in the soil–plant–atmosphere continuum and for identifying strategies that balance olive production with water conservation in semi-arid regions.

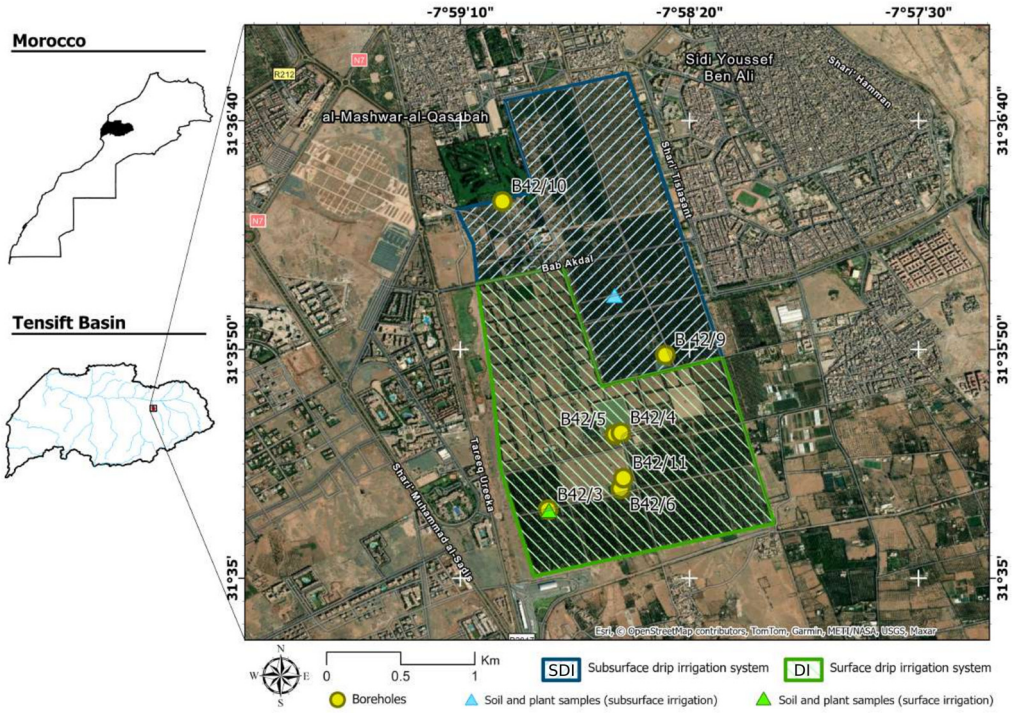

Figure 1. Location of the study area (Royal Domain of Agdal) east of Marrakech (Tensift Basin) highlighting the two experimental fields: surface drip irrigation DI (green hatching) and subsurface-drip irrigation SDI (blue hatching). Wells with groundwater access are shown as yellow circles; soil- and plant-sampling points are marked within each plot.

2.2. Sampling Protocol

The fieldwork was conducted in the Agdal olive orchards, where olive trees are irrigated using two distinct drip systems: surface (DI) and subsurface (SDI). These sites were selected to examine how irrigation methods influence water fluxes within the soil–plant–atmosphere continuum (SPAC). To capture the full range of water inputs and outputs, a comprehensive sampling strategy was implemented over a hydrological year (23 June 2022–23 June 2023).

The DI site used water from the 42/3 well, the primary source for surface irrigation, with 81 samples collected regularly to monitor variations in groundwater isotopic composition. This allowed for detailed analysis of temporal fluctuations potentially linked to irrigation schedules, rainfall, or broader hydrological processes. In contrast, the SDI site's 42/10 well was sampled only once, offering a limited but still valuable isotopic profile of the subsurface irrigation source.

Thirty precipitation samples were collected daily on rainy days using automatic water samplers, which were filled with paraffin oil to prevent evaporation before they reached the laboratory [29]. Irrigation water was sampled every other day to match its application schedule, allowing for the detection of short-term isotopic fluctuations. During this study, sixty-seven soil samples were taken monthly at four depths: 5 cm, 10 cm, 30 cm, and 50 cm using a hand auger. These depths were chosen to represent near-surface processes, as well as deeper infiltration and potential root uptake zones, with particular relevance to comparing surface and subsurface irrigation. By maintaining fixed depth increments, the sampling protocol ensured consistent and comparable snapshots of soil water content

and isotope ratios throughout the year. The soil samples were collected in very thin small plastic bags, then stored in a field cooler at a cold temperature before being transferred to the refrigerator at 4 °C until the day of extraction. Monthly plant samples were also collected: 18 branches and 16 leaves of the olive trees were harvested destructively, sealed promptly, and transported under chilled conditions. In the laboratory, the plant material was likewise placed in glass tubes and stored frozen (−0 °C). For both soil and plant samples, this procedure ensured sealed storage without grinding or open-air handling, thereby minimizing evaporation and isotopic fractionation prior to extraction.

2.3. Laboratory Analysis

All soil and plant samples underwent water extraction at the National Center for Energy Sciences and Nuclear Techniques (CNESTEN) laboratory using a cryogenic vacuum distillation system, a technique widely regarded as a gold standard for preserving original isotopic signatures [30]. In this method, the samples were first ground to increase surface area, then covered with a small amount of glass wool to prevent contamination, sealed in airtight glass flasks, labeled, tightly sealed with screw caps, and frozen until processing. For extraction, the sample tubes were assembled with empty trapping tubes and then shielded for 3 min in a cold trap, cooled with liquid 2-propanol at approximately −60 °C to reduce water vapor in the gas phase during evacuation. The entire setup was connected to a high-capacity vacuum pump to lower the pressure, effectively reducing the boiling point of water and allowing it to evaporate at relatively low temperatures (90–120 °C). This careful temperature control ensures that water is liberated without breaking down organic molecules or causing significant isotopic fractionation. Afterward, the sample tube was placed on a block heater while the water collection tube remained immersed in the cold trap. Distillation was carried out at 100 °C for 2 h. At the end of the process, the distillation assembly was vented, opened, and closed to allow any ice to melt. Finally, the collected water was pipetted into 2 mL sample vials, with a 0.3 mL insert used, if necessary, for stable isotopic analysis. To ensure reliability, soil extractions were performed in duplicate, which allowed us to assess the consistency of the isotopic signatures obtained. While full triplicates were not conducted for all samples, duplicates provided sufficient reproducibility, and any variability was within the analytical precision of the isotope measurements. The reported extraction efficiency (>98%) is based on earlier validation studies of the CVD [31], and our duplicate runs confirmed that our results remained within this range of accuracy for both $\delta^{18}O$ and $\delta^{2}H$ [31].

Water samples from precipitation, irrigation, soil, and groundwater were analyzed at the UM6P (University Mohammed 6 Polytechnic) laboratory using a Picarro L2140i cavity ring-down spectrometer (CRDS) (Picarro, Santa Clara, CA, USA). The measured $\delta^{18}O$ and $\delta^{2}H$ values were expressed in per mil with respect to Vienna Standard Mean Ocean Water (VSMOW) as follows in Equation (1):

$$\delta = \left(\frac{R_{sample}}{R_{standart}} - 1 \right) \times 1000‰ \quad (1)$$

where R_{sample} and $R_{standard}$ are the ratios of $^{18}O/^{16}O$ or $^{2}H/^{1}H$ in the sample and the standard (VSMOW), respectively. The precision of the measurements was ±1.0‰ for $\delta^{2}H$ and ±0.1‰ for $\delta^{18}O$. To avoid isotopic biases in plant water extracts (i.e., branch xylem and leaves), isotopic analyses were conducted at WSL Birmensdorf (Swiss Federal Institute for Forest, Snow, and Landscape Research) isotope laboratory using a thermal conversion elemental analyzer coupled to an DeltaXP isotope ratio mass spectrometer (TC/EA-IRMS, all Thermo Finnigan, Bremen, Germany). The precision of the WSL laboratory analysis is ±0.8‰ for $\delta^{2}H$ and ±0.1‰ for $\delta^{18}O$. From these paired isotopic measurements, we also

calculate the deuterium-excess parameter, d = $\delta^2H - 8 \cdot \delta^{18}O$. Because d-excess is sensitive to non-equilibrium processes such as evaporation, it provides a complementary line of evidence for distinguishing between source water signatures and evaporative enrichment along the soil–plant–atmosphere continuum. Together, $\delta^{18}O$, δ^2H, and their derived d-excess constitute the core dataset that will be used to trace water movement and quantify evaporation in the two irrigation layouts examined here.

3. Results and Discussion

3.1. Description of $\delta^{18}O$ and δ^2H for Different Waters

3.1.1. Rainwater

The stable isotopic composition of the rainfall collected in the study area during the period of the sampling varies within a wide range from −13.1‰ to −2.66‰ and from −91.2‰ to −0.2‰ for $\delta^{18}O$ and δ^2H, respectively (Figure 2). The lowest isotope values are recorded during February 2022. Figure 2 shows that the rainwater samples fell above the global meteoric water line (GMWL: $\delta^2H = 8 \times \delta^{18}O + 10$) [22], and around the local meteoric water line (LMWL: $\delta^2H = 8 \times \delta^{18}O + 13.7$) performed by Raibi in 2006. This indicates a mixed Atlantic and Mediterranean origin of the air masses that generate the precipitation in the study site with a little evaporation. This interpretation is further supported by the d-excess values, which remain close to +13‰, consistent with moisture sources influenced by both marine and continental conditions, and more specifically pointing to a predominantly Mediterranean origin.

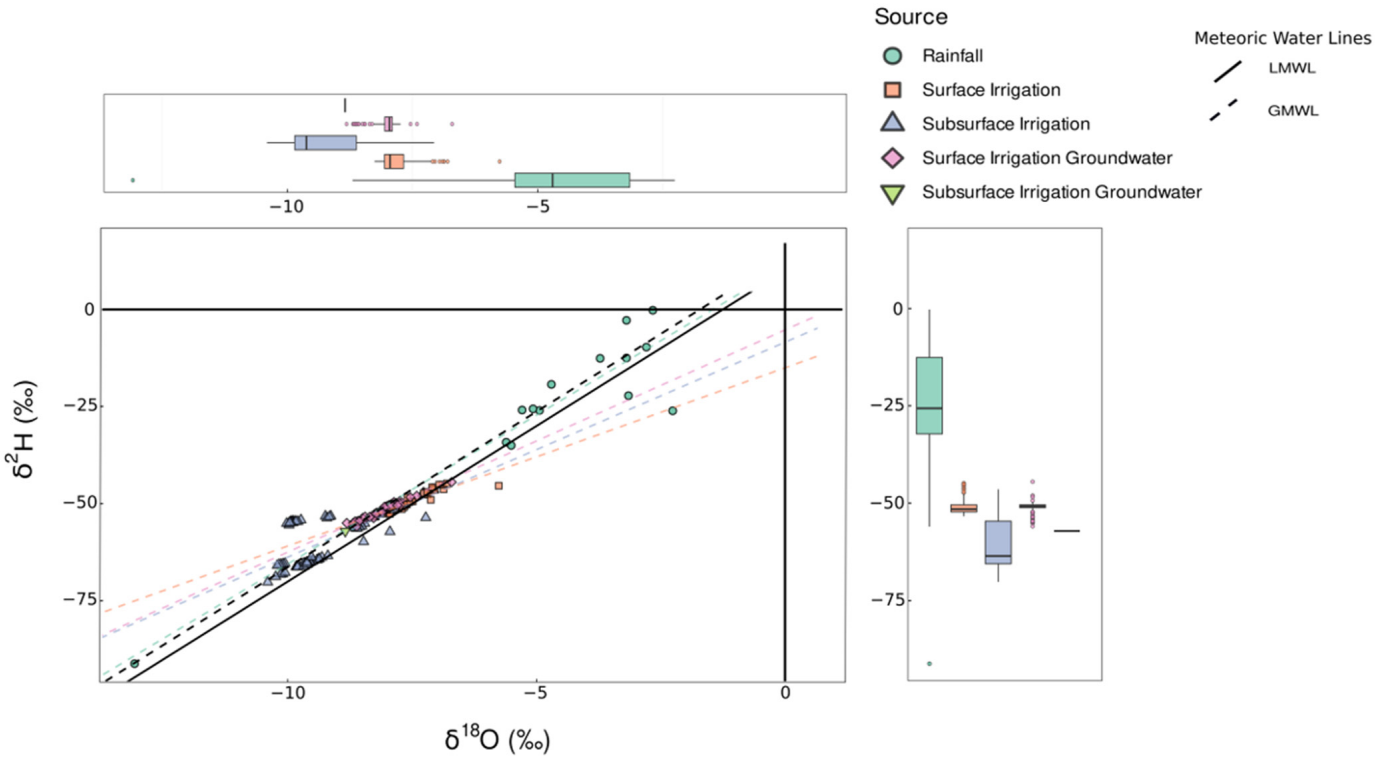

Figure 2. Dual-isotope plot ($\delta^{18}O$ vs. δ^2H) illustrating the isotopic composition of multiple hydrological compartments (rainfall, groundwater, irrigation water) relative to the global meteoric water line (GMWL) and local meteoric water line (LMWL).

3.1.2. Irrigation Water

Irrigation water samples were collected from two open storage basins, each one fed by the aforementioned wells and dedicated to one of the surface (DI) or subsurface drip (SDI)

irrigated plots. The basins occasionally receive river water from a traditional canal called *Taseltant* (Figure 3), which diverts water from the Ourika river at the mountain-front.

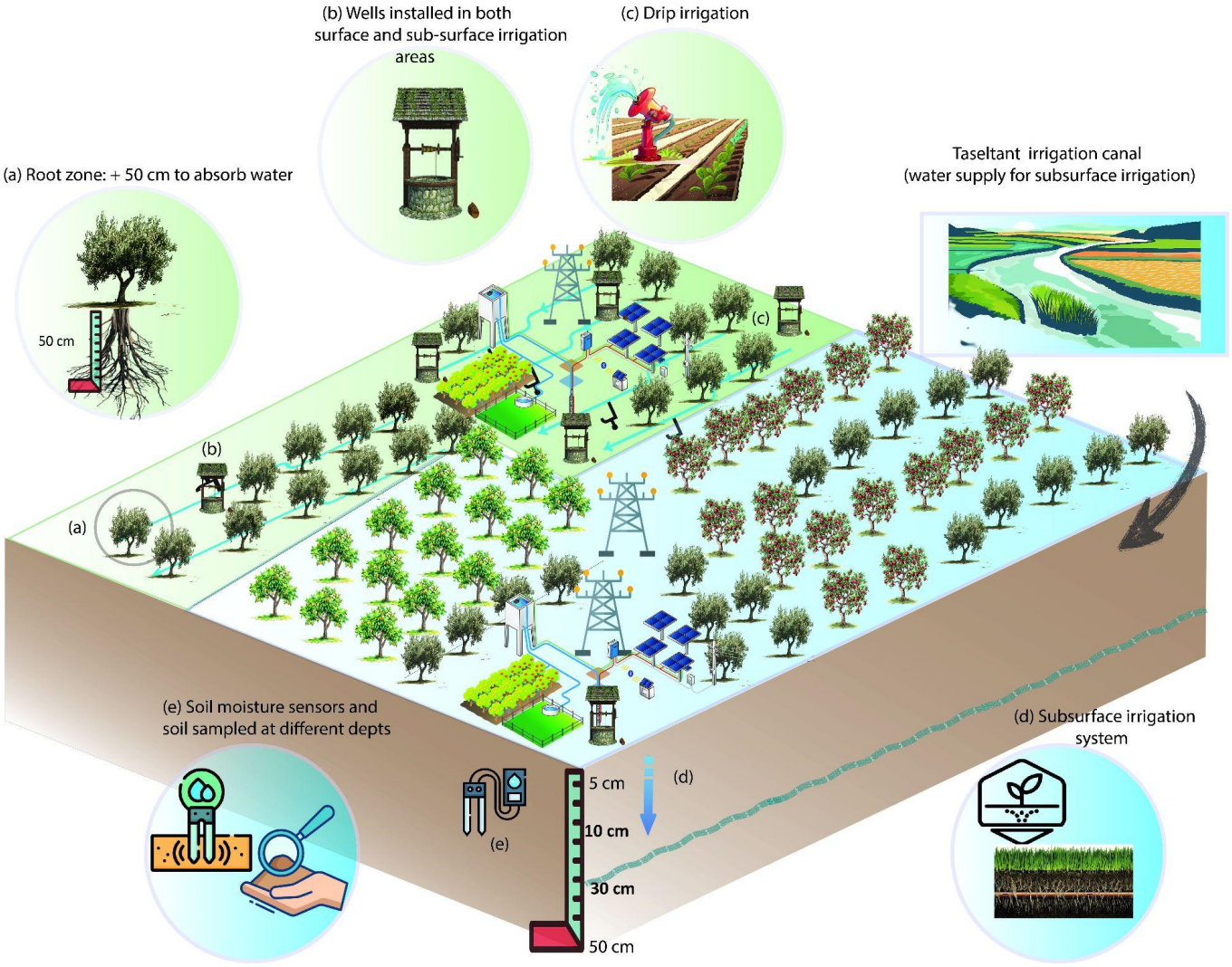

Figure 3. Schematic overview of the experimental olive orchard setup showing key components for monitoring water dynamics under surface and subsurface irrigation systems. The design includes olive trees, drip and subsurface irrigation systems, and soil isotope sampling at multiple depths.

The isotopic composition of surface irrigation water ranged from −8.23‰ to −5.76‰ and from −53.3‰ to −45.4‰ for $\delta^{18}O$ and $\delta^{2}H$, respectively, while subsurface irrigation samples ranged from −10.41‰ to −7.07‰ and from −70.2‰ to −46.4‰, for $\delta^{18}O$ and $\delta^{2}H$, respectively (Figure 2). The isotopic composition of irrigation water splits into two distinct groups with the subsurface irrigation group being more depleted in heavy isotopes than the surface irrigation group (Figure 4). Both groups fell between the global and local meteoric water lines with a slight evaporation effect. The surface irrigation group had a similar isotopic signature to its corresponding groundwater samples (Figure 2) with a slight evaporation effect probably caused by the residence time at the storage basin after pumping. Subsurface irrigation group is more depleted than its groundwater source (Figure 2) indicating that it may come from the other well where we only had one sample (42/10), or that may originate from the Taseltant canal (Figure 3).

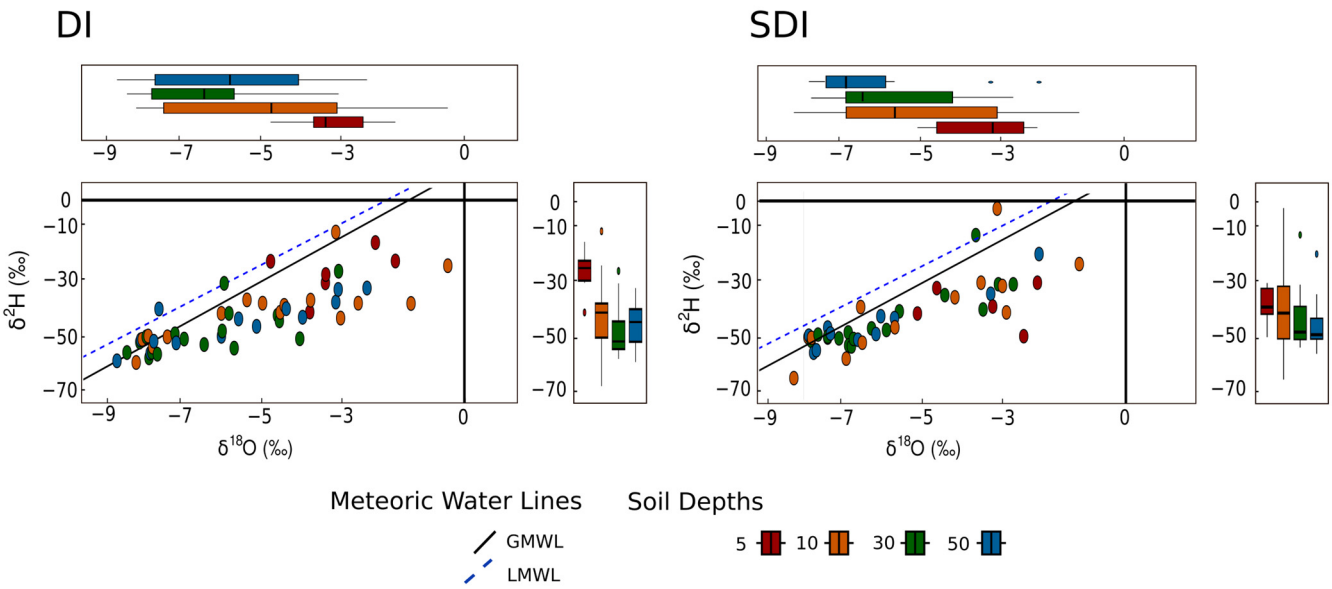

Figure 4. Dual-isotope plot ($\delta^{18}O$ vs. $\delta^{2}H$) of soil water from different depths (5, 10, 30, and 50 cm) for (**DI**) surface irrigation site (on the (**left**)) and (**SDI**) subsurface irrigation site (on the (**right**)).

3.1.3. Groundwater

The isotopic composition of groundwater supplying in DI (well 42/3) ranged from −8.8‰ to −6.7‰ and from −55.1‰ to −44.5‰ for $\delta^{18}O$ and $\delta^{2}H$, respectively (Figure 2), The groundwater isotope signatures are mainly scattered toward depleted values, with slight evaporation, that could be explained by recharge seasonality. For SDI, we only had one sample of the 42/10 well, with values of −57.1‰ and −8.85‰ for $\delta^{2}H$ and $\delta^{18}O$, respectively. This depletion could be attributed to the altitude of recharge, which controls groundwater in the Haouz aquifer because of water sourced from the High-Atlas Mountain. Indeed, the difference between the groundwater signature and the local rain signature confirms that groundwater recharge at the study site is not direct but rather occurs indirectly through high-elevation sourced water [32].

3.1.4. Soil Water

Soil samples were collected at four depths (5 cm, 10 cm, 30 cm, and 50 cm) to capture $\delta^{18}O$ and $\delta^{2}H$ across the soil profile, especially the shallow layers (<10 cm) where strong seasonal dynamics and evaporative effects are expected. Sampling at deeper layers (30 and 50 cm) allowed the assessment of more stable soil water pools, although collecting samples beyond 50 cm was constrained due to the use of a hand auger in the arid soil conditions. Nevertheless, significant isotopic variation was anticipated due to the strong vertical evaporation gradient typical of arid and semi-arid soils. The isotopic composition varied with both soil depth and irrigation type. Within the soil profile, $\delta^{18}O$ ranged from −8.41‰ to −1.15‰, and $\delta^{2}H$ from −59.8‰ to −19.6‰, in the DI (surface irrigation) site, while $\delta^{18}O$ ranged from −8.66‰ to −2.15‰ and $\delta^{2}H$ from −59.2‰ to −23.3‰, in SDI (subsurface irrigation). When considered separately (Figure 4), both sites display vertical isotopic depletion with increasing depth, consistent with decreasing evaporative enrichment. Average $\delta^{18}O$ values decreased from −3.39‰ at 5 cm to −6.48‰ at 50 cm across all samples, reflecting the effect of kinetic fractionation, whereby lighter isotopes preferentially evaporate, enriching the remaining soil water in heavier isotopes [33].

Despite the general trend, substantial isotopic variability between the various depths is observed in both the irrigation systems, particularly at 10 cm, where $\delta^{18}O$ ranges from less than −8‰ to more than −1‰, and $\delta^{2}H$ ranges from below −60‰ to above −20‰This

wide spread suggests that evaporation strongly influenced the upper soil layers, likely extending beyond the surface into the top 10–20 cm, regardless of irrigation method. Previous studies have reported similar patterns, with isotopic fractionation influencing the top 50 cm of soil in Mediterranean climates [34] and up to 3 m in arid environments [35,36].

The large isotopic range is also attributable to the mixing of waters with contrasting isotopic signatures: enriched precipitation (e.g., $\delta^{18}O \approx -4.9‰$, $\delta^{2}H \approx -26.6‰$) and more depleted groundwater and surface irrigation water (e.g., $\delta^{18}O \approx -8.0‰$, $\delta^{2}H \approx -51.1‰$). Notably, the SDI treatment shows slightly more depleted values at depth compared to DI, likely due to reduced surface evaporation from buried water inputs and possibly greater reliance on deeper, less fractionated water sources.

3.1.5. Plant Water

The isotopic composition of plant water from the olive trees, including both branch xylem and leaf samples, differed between irrigation treatments and reflects the influence of evaporative processes and water source availability (Figure 5). DI Branch xylem water $\delta^{18}O$ ranged from −5.79‰ to 9.03‰ and $\delta^{2}H$ from −51.44‰ to 14.29‰ under the DI treatment, while leaf water values ranged from −4.79‰ to 13.02‰ for $\delta^{18}O$ and from −46.11‰ to 30.33‰ for $\delta^{2}H$. In contrast, the SDI treatment showed narrower, more depleted isotopic ranges with bch xylem $\delta^{18}O$ ranging from −2.76‰ to 6.12‰ and $\delta^{2}H$ from −27.33‰ to 11.68‰, and leaf water $\delta^{18}O$ from −2.16‰ to 7.44‰ and $\delta^{2}H$ from −22.92‰ to 16.59‰.

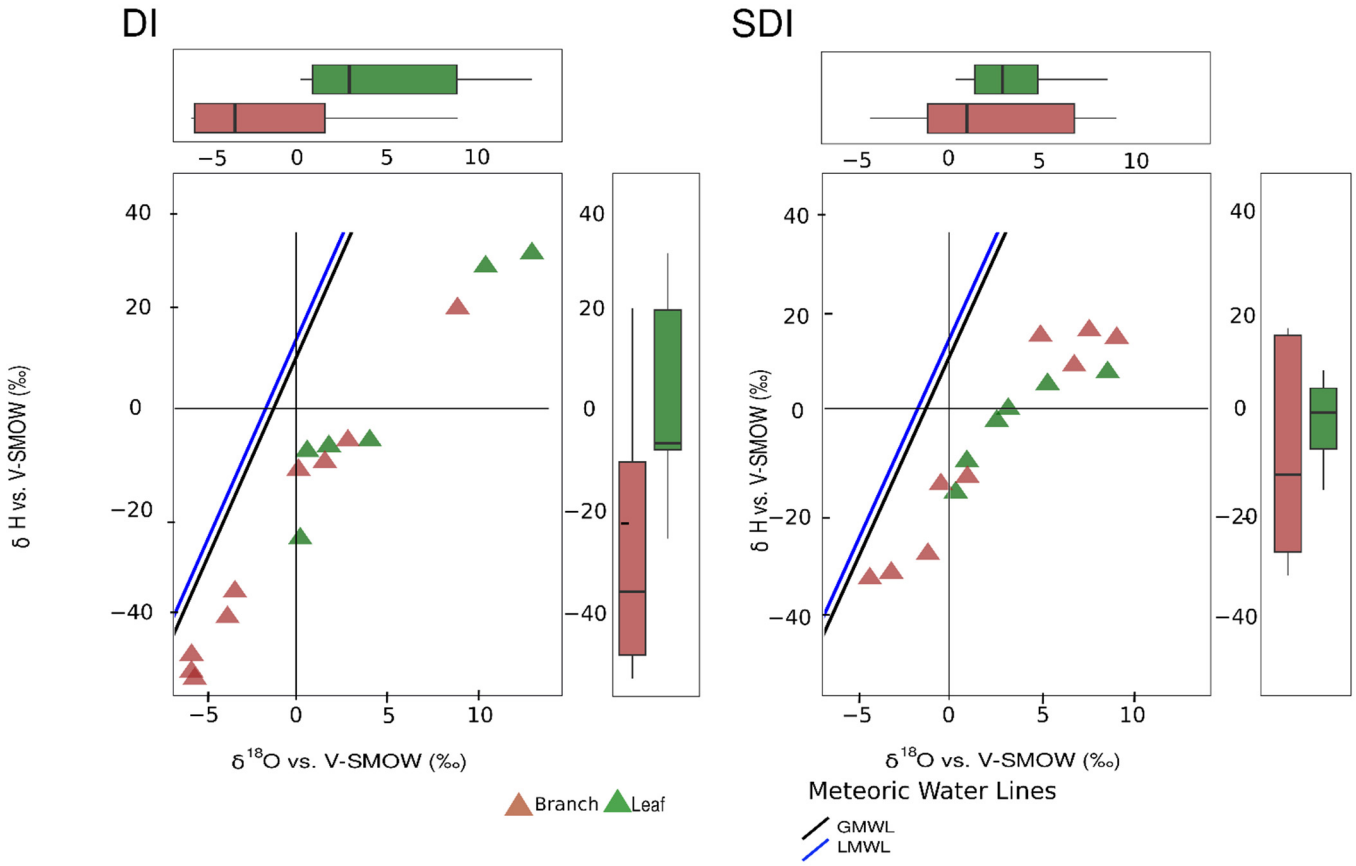

Figure 5. Dual-isotope plot ($\delta^{18}O$ vs. $\delta^{2}H$) of branch xylem and leaf water for DI (**left**) and SDI (**right**).

In both treatments, leaf water was on average more enriched in heavy isotopes than branch water, consistent with transpirative enrichment due to kinetic fractionation occurring at the leaf level. This is particularly evident in DI, where the greater isotopic range and higher enrichment suggest stronger evaporative demand and a higher degree of post-uptake fractionation. The evaporation trend of plant water intersects the LMWL both in

DI and SDI treatment, but the slope is more acute in SDI, indicating that under subsurface irrigation, plant uptake is dominated by isotopically more stable water likely sourced from deeper, less evaporated zones. This is consistent with findings by Orlowski et al. [37], who reported that irrigation method and water residence time in the soil can significantly influence isotopic source water signatures. In contrast, DI shows greater deviation from the LMWL and a wider spread in both $\delta^{18}O$ and $\delta^{2}H$, pointing to greater evaporative enrichment and likely root uptake of near-surface water affected by fractionation. The observed isotopic variability between DI and SDI reflects the physical configuration of the irrigation systems. In SDI, water is delivered at 30 cm, reducing surface exposure and evaporation, thus maintaining lower isotopic values and tighter clustering. In DI, the shallow application of irrigation water increases its exposure to atmospheric demand, enhancing isotopic enrichment before uptake. Similar effects have been documented in controlled experiments by Barbeta et al. [38], who demonstrated that soil surface evaporation can strongly influence the isotopic signature of xylem and leaf water, especially in trees accessing shallow soil water. The isotopic distinction between plant compartments (leaf vs. branch) and irrigation treatments illustrates the integrated effects of plant water uptake strategy, irrigation configuration, and soil evaporation.

3.2. Relationships Between Soil Water and Plant Water: Implications for Root Water Uptake of Olive Trees

The similarities between the isotopic composition of soil water and plant xylem can be used to infer the plant root water uptake depth, thus, assessing plant water use strategies under different environmental conditions [36]. This approach rests on two key assumptions: (i) minimal or no isotopic fractionation during water transport from roots to xylem, and (ii) a discernible isotopic gradient in the soil profile. In the DI treatment with surface emitters, the soil gradient is faint: $\delta^{18}O$ values at 10 cm and 50 cm overlap within analytical uncertainty (Figure 4), suggesting intense mixing of surface-applied water. Branch xylem nevertheless spans −6‰ to 0‰ $\delta^{18}O$ and overlaps the soil field (Figure 5), so olives still rely on the first half meter; however, the blurred gradient masks a single dominant uptake depth. Leaves are again more enriched than branches, but the offset is smaller than under SDI, reflecting the lower evaporative demand during the DI sampling window.

The SDI layout, where emitters are buried at ~30 cm, tells a different story. The soil profile displays a depletion of heavy isotopes: median $\delta^{18}O$ falls from roughly −3‰ at 5 cm to almost −7‰ at 50 cm, with a parallel decline in $\delta^{2}H$ (Figure 4). Branch xylem samples plot inside the same envelope, confirming that roots tap the entire 0–50 cm layer but most actively the 5–30 cm zone around the emitters, as indicated by two autumn clusters centered on −5.7‰ and −3.6‰ $\delta^{18}O$. Leaves collected at the same times are markedly more enriched (0 to +10‰ $\delta^{18}O$, up to +30‰ $\delta^{2}H$), falling well above the local meteoric water line; this is the classic evaporative signature of water that has traveled from xylem to the leaves. A third, midsummer branch cluster averaging +0.7‰ $\delta^{18}O$ lies even further along the evaporation line than any sampled soil, implying that under peak atmospheric demand some roots shift to the highly evaporated 0–5 cm layer rather than any fractionation within the plant, a process shown to be minimal in olives [39].

But these three clusters are also shown in DI, in which we can deduct other assumptions: (i) these samples are either sourced from the soil layer less than 5 cm, subject to higher evaporation influence; (ii) have been subject to additional evaporation during transport from roots to branches; or (iii) the pattern could simply reflect an artifact introduced during sampling, transport, or extraction.

Figure 6 compresses the entire soil–plant–atmosphere continuum into a single dual-isotope view, revealing that every water pool, rainfall, irrigation, soil layers, branch xylem and leaves, lies along one shallow-slope evaporation trajectory that branches off the lo-

cal meteoric water line whether on DI or SDI; the kinetic process is thus common across treatments, while the distance each pool travels along that line records how much evaporation it has endured. Rainfall and groundwater cluster tightly on the meteoric line, confirming negligible pre-infiltration enrichment; SDI water coincides with this meteoric cluster, whereas DI is already about 1–2‰ heavier in $\delta^{18}O$, nudging all subsequent DI points rightward before field evaporation even begins. Shallow DI soils (0–10 cm) extend furthest along the trajectory to nearly +5‰ $\delta^{18}O$, signaling repeated wet–dry cycles at the surface, while SDI soils, wetted at 30 cm depth, remain within +2‰ of rainfall and therefore occupy an up-gradient, less-evaporated position. Branch xylem samples from each treatment sit comfortably inside the isotopic envelope of their respective 0–50 cm soil profiles, indicating that olive roots draw a depth-integrated blend of available soil water without additional fractionation, and leaves then shift a further 3–5‰ along the same line through transpiration, with the DI canopy reaching the extreme enrichment seen in its topsoil whereas SDI leaves never attain such values. This stepped progression—rainfall → irrigation → soil → branch → leaf, forms a visible isotopic "ladder" whose rungs are widely spaced under surface drip but compressed under subsurface drip, illustrating that burying emitters shortens the evaporation path, limits non-productive water loss, and ultimately supplies the trees with isotopically cooler, more efficient water, beyond simply showing the expected enrichment of plant water, underscoring the actual sources of water used by trees under different irrigation regimes.

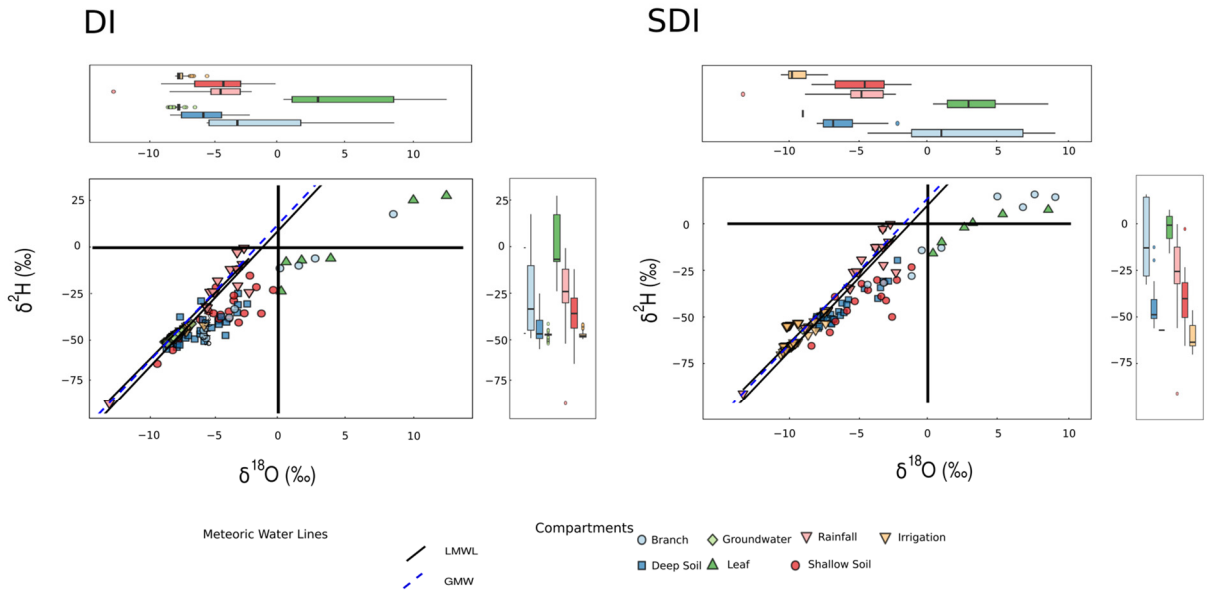

Figure 6. Dual-isotope plot ($\delta^{18}O$ vs. $\delta^{2}H$) displaying the isotopic composition of rainfall, groundwater, surface irrigation water, subsurface irrigation water, soil water (various depths), and olive plant water (leaves, branches). The black line (GMWL) and dark blue dashed line (LMWL) represent meteoric water lines, while the green line indicates the soil evaporation line.

3.3. Seasonal Variation in Plant Xylem and Soil Water

Seasonal changes in plant xylem and soil water $\delta^{18}O$ exhibit distinct patterns in DI and SDI systems (Figure 7). Winter values remain stable in both systems, reflecting infiltration of isotopically depleted precipitation [40]. Summer brings significant enrichment, particularly in DI surface soils due to evaporative fractionation, with xylem water mirroring this trend. SDI systems maintain more depleted values through subsurface water delivery [20]. The spring peak in DI plant (branches and leaves) $\delta^{18}O$ (exceeding summer values by 1–2‰) likely results from combined ecohydrological and methodological factors: (1) transient preferential uptake of evaporatively enriched shallow water during root system activation,

and (2) potential analytical artifacts from cryogenic extraction that may amplify early-season enrichment [16]. Autumn shows intermediate values as trees transition to deeper sources. The more significant $\delta^{18}O$ variability in DI (15‰ range vs. 10‰ in SDI) highlights its more substantial evaporation exposure and shallower water sourcing compared to stable isotopic profile of SDI. These patterns demonstrate how irrigation methods fundamentally alter soil–plant water dynamics in semi-arid ecosystems.

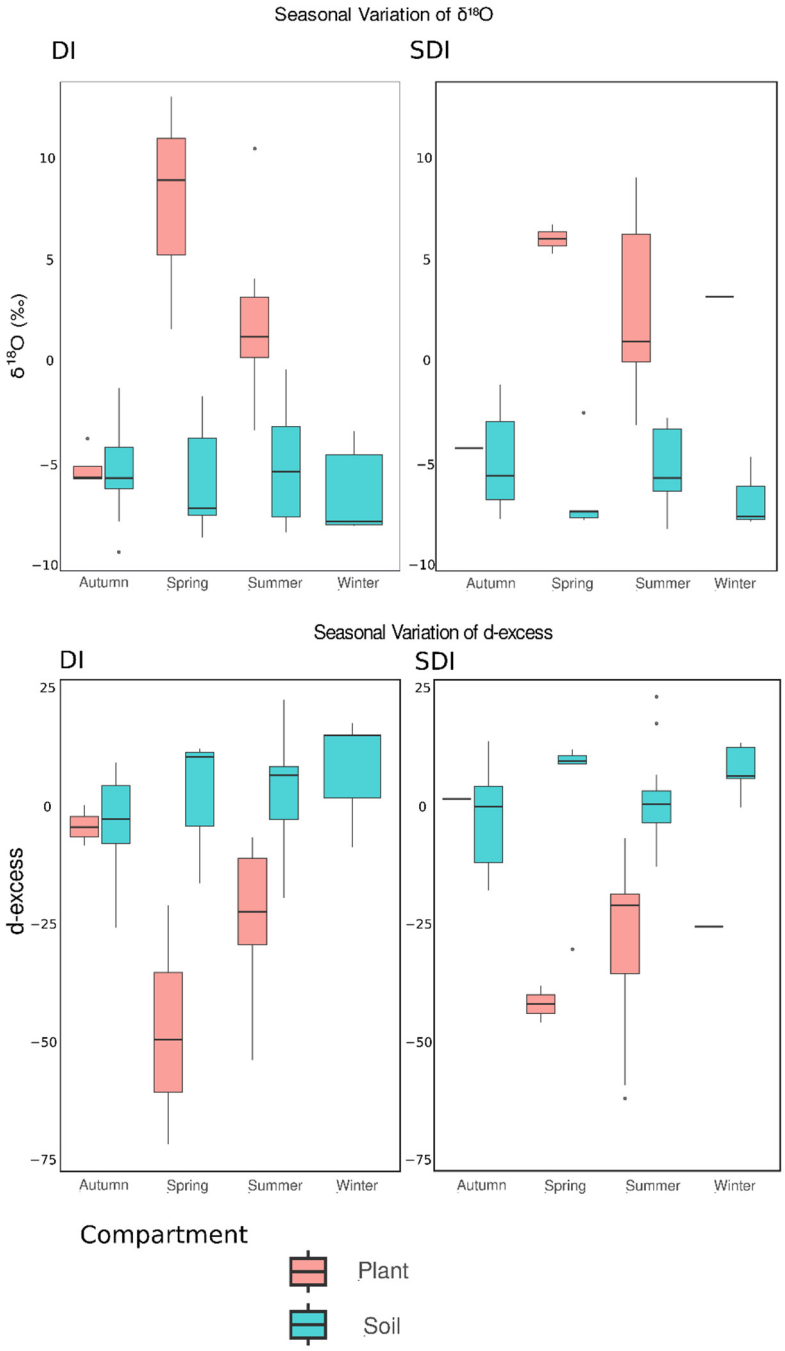

Figure 7. Seasonally grouped distributions of in $\delta^{18}O$ (‰) (**top**) and d-excess (**bottom**) values measured in plant water (red) and soil water (blue, merging all depths) in the surface (**left panels**) and subsurface (**right panels**) irrigation systems.

In Figure 7, the subsurface irrigation system (SDI) shows soil water d-excess maintaining consistently positive values throughout the year, especially during winter and spring. This stability indicates minimal evaporative influence and a predominant contribution from meteoric water inputs. During summer, a slight decline in d-excess suggests limited evapora-

tive enrichment, underscoring the effectiveness of subsurface water delivery in mitigating evaporation. Conversely, in the surface irrigation system (DI), soil water d-excess exhibits greater seasonal variability. Moderately elevated positive values in winter and spring reflect recharge by precipitation that carries a typical Mediterranean d-excess of roughly +8 to +12‰, and infiltrates with minimal post-events evaporation, while a slight decrease during summer points to significant evaporative enrichment of surface-applied water.

The isotopic composition of branch water reflects the combined influence of source water uptake and post-uptake fractionation processes, though it is not possible to clearly distinguish between xylem and leaf water in the graph. In SDI, plant water d-excess remains relatively stable with a median of roughly −25‰ in summer, with a wide spread down to −60‰. This negative drop of d-excess means that the water has already undergone kinetic evaporation, where ^{18}O is retained preferentially over ^{2}H, either (i) before uptake in near-surface soil that partially dried, or (ii) after uptake through leaf-level fractionation that back-diffuses into the xylem. While in DI, plant water d-excess exhibits clear seasonal variation. During summer, markedly negative d-excess values point to increased reliance on shallow, evaporatively enriched soil water. The high level of enrichment, possibly influenced by leaf water signatures, reflects intensified transpiration under hot, dry conditions. These patterns are consistent with recent studies that report seasonal shifts in plant water isotopic signatures, highlighting the impact of soil enriched water in shaping water uptake and evaporative dynamics [41].

The inverse relationship between d-excess and $\delta^{18}O$ further elucidates the effects of evaporation and water source changes. During summer, increased $\delta^{18}O$ values coupled with increasingly negative d-excess in soil, branch, and leaf water under DI indicate substantial evaporative enrichment and a shift towards the use of shallower water sources. In SDI, the relatively stable $\delta^{18}O$ and d-excess values suggest that subsurface irrigation effectively buffers against seasonal isotopic shifts, maintaining access to deeper, isotopically consistent water. The stability of d-excess and $\delta^{18}O$ in SDI suggests that subsurface irrigation provides a more reliable water source, reducing evaporative stress and enhancing drought resilience. Similar stability has been documented in Alpine orchards irrigated with buried drip lines, where soil and xylem d-excess stayed within +2 to +9‰ despite summer heat waves [42]. Conversely, the pronounced seasonal isotopic shifts observed in DI mirror the large summer enrichment ($\delta^{18}O \approx +8$‰; d-excess ≈ -30‰) found under surface-spray irrigation in European apple orchards [43], underscoring the evaporative losses inherent to surface delivery. These observations reinforce the broader European consensus that SPAC-scale isotope monitoring is a powerful tool for designing water-saving irrigation strategies [43].

3.4. Limitations and Perspective

Our research identified substantial alterations in isotopic behavior under surface (DI) and subsurface (SDI) drip irrigation in a semi-arid orchard system, notwithstanding numerous technical and conceptual challenges. The differentiation of plant and soil isotope data between the two irrigation treatments indicated that surface irrigation (DI) consistently yielded more enriched and variable $\delta^{18}O$ and $\delta^{2}H$ values in both soil and plant compartments, especially in upper soil layers and leaf water, thereby underscoring the significant impact of evaporative enrichment. Subsurface irrigation (SDI) had a more reduced and less variable isotopic signature, indicating a more stable water source from deeper, less evaporation-affected regions. Although the plot-scale isotope patterns clearly separate surface (DI) from subsurface (SDI) drip irrigation, several methodological constraints blur fine-scale interpretation. First, the point-source geometry of drip emitters promotes lateral redistribution and preferential flow; as a result, soil water collected 10 cm below

an emitter can share the same $\delta^{18}O$–$\delta^{2}H$ signature as water sampled 50 cm deep even though the two parcels followed distinct flow paths [44]. Second, our fortnightly, bulk-core sampling relies on cryogenic vacuum extraction, a technique known to co-extract tightly bound pore water whose isotope composition differs from the mobile fraction accessed by roots, thereby dampening vertical gradients [37]. Third, recent syntheses show that xylem water may undergo within-plant fractionation or mix with leaf back-diffusion, meaning that "stem ≙ source" is not always valid and can further obscure depth assignment [45]. Moreover, there exists additional uncertainty due to potential isotopic alterations during sample preparation and storage. Despite the samples being chilled prior to cryogenic extraction, the interval between sampling and analysis likely resulted in significant isotopic fractionation, particularly in the drier topsoil samples characteristic of DI. Zhang et al. [46] and Amin et al. [39] emphasize that conventional cryogenic extraction methods are susceptible to bias in soils with low moisture or high organic content. Employing in situ vapor equilibration techniques or dual-method comparisons, such as cryogenic versus centrifugation procedures, may improve extraction accuracy [47,48]. To provide robust isotopic datasets, recent quality-control guidelines advocate for the assessment of extraction efficiency and reproducibility across varied samples [49]. Taken together, these factors explain the overlapping $\delta^{18}O$ and $\delta^{2}H$ ranges we observed between 10 cm and 50 cm and caution against using the present dataset to locate root water uptake zones. Future work combining in situ isotope probes, high-resolution soil-moisture sensing and tracer-pulse experiments would help disentangle these processes while retaining the robust treatment-level contrast documented here. Furthermore, isotope-based mixing models like MixSIAR or SIAR can offer valuable tools for estimating the proportions of shallow versus deep soil water contributing to plant uptake. However, the reliability of Bayesian mixing models hinges on how clearly separated the isotopic signatures of the potential sources are. In our study, there is significant overlap between the 10–50 cm soil horizons, which means it would be necessary to (i) group individual depths into broader categories representing 'shallow' and 'deep' sources, and (ii) incorporate informed priors derived from data on root distribution and soil moisture dynamics. When these conditions are met, MixSIAR has been shown to outperform simpler iso-source approaches in semi-arid cropping systems [12] and has proven effective in flooded rice fields when priors are applied [50].

In our context, these approaches may assist in ascertaining whether the observed enrichment in DI leaves signifies shallow water uptake or post-uptake fractionation, concerns particularly relevant in water-scarce agricultural settings. Prior research by Zhao et al. [51], and Rothfuss & Javaux [52] substantiates this approach by illustrating the application of plant and soil isotope signatures to model seasonal and depth-dependent root water uptake in Mediterranean and semi-arid environments where our findings confirm a broader consensus: isotope-based SPAC diagnostics must be more extensively integrated into routine agricultural monitoring to enhance irrigation efficiency and sustainability. Recent advancements in technology, particularly field-deployable laser spectroscopy devices like CRDS and OA-ICOS, enables high temporal resolution measurements of water isotopes in soil and plant compartments [45]. While these systems diminish the necessity for laboratory analysis and may detect quick variations in isotopic signals, they nevertheless demand substantial on-site infrastructure, frequent maintenance, and specialized technical knowledge. When combined with remote sensing and soil moisture data, these techniques offer potential for enhancing irrigation scheduling by delivering insights into actual plant water uptake dynamics, rather than depending exclusively on predicted soil moisture levels.

4. Conclusions and Implications

In this study, we examined the movement of irrigation water in the SPAC in olive tree plots in semi-arid conditions under two irrigation systems: surface drip (DI) and subsurface drip with drip laterals buried at 30 cm (SDI). We analyzed samples of precipitation, soil, plant, and irrigation water for stable water isotopes ($\delta^{18}O$, $\delta^{2}H$). By tracking the seasonal variation in distinct rainfall and irrigation water isotope signatures through the 0–50 cm profile and into xylem, we found that three consistent patterns emerged as follows: (i) the subsurface drip (SDI) maintained narrower and more depleted isotope ranges below approximately 20 cm, signaling deeper and more stable wetting fronts; (ii) branch water under SDI exhibited significantly less evaporative enrichment compared to that under DI, suggesting a closer connection between irrigation pulses and active root zones; (iii) under surface drip system (DI), isotope transients only propagated to about 15 cm, and branch water showed strong enrichment, indicating greater near surface evaporation and percolation losses.

Our findings underscore the diagnostic potential of stable isotopes to reveal changes in plant–soil interactions under various irrigation systems, despite the persistence of isotopic errors related to sampling depth and methodological consistency. The results showed that subsurface drip irrigation (SDI) mitigates seasonal isotopic fluctuations and limits evaporative enrichment in branch water compared to surface drip (DI), indicating a more stable and efficiently targeted root water supply in semi-arid orchards. Ultimately, this confirms SDI as a practical lever to reduce non-productive losses and to enhance irrigation to achieve deeper, better timed wetting fronts.

More broadly, our isotope approach turns "where plants actually drink" into a measurable management metric, paving the way for evidence-based irrigation design and scheduling. Future research should include routine isotope checks at additional strategic depths (1 m and beyond) during peak demand, paired with continuous soil moisture and sap flux monitoring to quantify real water savings under various irrigation regimes. Furthermore, to move beyond merely descriptive isotope patterns, isotope time series can be embedded within Bayesian mixing frameworks, such as MixSIAR, to statistically analyze depth-specific contributions to root water uptake. Concurrently, assimilating the same dataset into isotope-enabled process models such as EcH2o-iso for coupled plant–soil exchange would convert qualitative enrichment patterns into explicit estimates of seasonal evapotranspiration partitioning, deep percolation, and groundwater recharge. This study demonstrates how continuous, compartment-resolved isotope monitoring can be operationalized to verify the active rooting depths targeted by irrigation and to identify when irrigation water is lost by near surface evaporation. This experimental study advances isotope hydrology and opens the door to real time, isotope-informed irrigation control and policy tools tailored to semi-arid agriculture.

Author Contributions: T.A.: Writing—original draft, visualization, methodology, investigation, field experimentation, lab work, formal analysis, data curation, and conceptualization. M.H.K.: Writing—review and editing, visualization, supervision, methodology, investigation, formal analysis, data curation, conceptualization, and project administration. S.K.: Writing—review and editing, visualization, validation, supervision, methodology, investigation, and formal analysis. Y.A.B.: Writing—review and editing, visualization, supervision, methodology, investigation, formal analysis, data curation, and conceptualization. L.B.: Writing—review and editing, visualization, supervision, methodology, investigation, and formal analysis. V.D.: Writing—review and editing, validation, and supervision. M.M.L.: Writing—review and editing, methodology, investigation, lab work, formal analysis, and data curation. F.R.: Writing—review and editing, visualization, supervision, methodology, investigation, lab work, formal analysis, data curation, and conceptualization. T.E.: Writing—original draft, visualization, supervision, methodology, investigation, lab work, formal analysis, data curation, and conceptualization. A.E.: Writing—review and editing, visualization,

investigation, field experimentation, and lab work. N.R.: Writing—review and editing, visualization, and conceptualization. H.B.: Writing—review and editing, visualization, methodology, investigation, and formal analysis. A.C.: Supervision, project administration, and funding acquisition. All authors have read and agreed to the published version of the manuscript.

Funding: This research was conducted in the frame of the ASSIWAT project (grant agreement no: AS_71) funded by the Office Chérifien des Phosphates (OCP Group S.A.). We would also like to thank the Moroccan Ministry of Higher Education, Scientific Research and Innovation and the OCP Foundation for their support through the APRD research program (GEANTech). M.M.L. is supported by the Swiss National Science Foundation (grants 213367 and 229377).

Data Availability Statement: The data presented in this study are not publicly available due to contractual and proprietary restrictions. The dataset is the property of OCP Group S.A., which funded this research, and its distribution is subject to confidentiality agreements. Access to the data may be granted upon reasonable request and with permission from OCP Group S.A.

Acknowledgments: We thank the managers of "Les domaines Agricoles" company for making their Agdal site available for this experiment and providing us with necessary data of the study site. Cryogenic vacuum distillation of soil water samples was conducted at CNESTEN (Centre National de l'Énergie, des Sciences et des Techniques Nucléaires), whose support is gratefully acknowledged. We warmly thank Tibari El ghali, Fatima Raibi, Manuela Oettli, and Matthias Saurer for their expert technical assistance in cryogenic vacuum distillation extraction of xylem and leaf samples and their subsequent isotopic analysis at the isotope laboratory of CNESTEN Rabat and WSL Birmensdorf.

Conflicts of Interest: The authors declare that this study received funding from OCP Group (AS_71). The funder was not involved in the study design, collection, analysis, interpretation of data, the writing of this article, or the decision to submit it for publication.

References

1. Matthews, J.B.R.; Möller, V.; van Diemen, R.; Fuglestvedt, J.S.; Masson-Delmotte, V.; Méndez, C.; Semenov, S.; Reisinger, A. Annex VII: Glossary. In *Climate Change 2021: The Physical Science Basis. Contribution of Working Group I to the Sixth Assessment Report of the Intergovernmental Panel on Climate Change*; Masson-Delmotte, V., Zhai, P., Pirani, A., Connors, S.L., Péan, C., Eds.; Cambridge University Press: Cambridge, UK; New York, NY, USA, 2021; pp. 2215–2256. [CrossRef]
2. Mekonnen, M.M.; Hoekstra, A.Y. Sustainability of the blue water footprint of crops. *Adv. Water Resour.* **2020**, *143*, 103679. [CrossRef]
3. Falkenmark, M.; Wang-Erlandsson, L. A water-function-based framework for understanding and governing water resilience in the Anthropocene. *One Earth* **2021**, *4*, 213–225. [CrossRef]
4. Ait Dhmane, L.; Saidi, M.E.; Moustadraf, J.; Rafik, A.; Hadri, A. Spatiotemporal characterization and hydrological impact of drought patterns in northwestern Morocco. *Front. Water* **2024**, *6*, 1463748. [CrossRef]
5. Mehta, P.; Siebert, S.; Kummu, M.; Deng, Q.; Ali, T.; Marston, L.; Xie, W.; Davis, K.F. Half of twenty-first century global irrigation expansion has been in water-stressed regions. *Nat. Water* **2024**, *2*, 254–261. [CrossRef]
6. Hamdy, A.; Ragab, R.; Scarascia-Mugnozza, E. Coping with water scarcity: Water saving and increasing water productivity. *Irrig. Drain.* **2003**, *52*, 3–20. [CrossRef]
7. Achli, S.; Ongoma, V.; Epule, T.E.; Dhiba, D.; Salih, W.; Ousayd, L.; Chehbouni, A. Exploring the key drivers of crop yields in Morocco—A systematic review. *Front. Agron.* **2025**, *7*, 1515938. [CrossRef]
8. Khabba, S.; Er-Raki, S.; Ezzahar, J.; Merlin, O.; Kharrou, M.H.; Chehbouni, A. Experimental assessment of irrigation efficiency over the dominant (flood and drip) irrigated crops in the Haouz plain, center of Morocco. *Acta Hortic.* **2025**, *1422*, 275–282. [CrossRef]
9. Attou, T.; Kuppel, S.; Kharrou, M.H.; Ezzahar, J.; Bouchaou, L.; Ait Brahim, Y.; Demarez, V.; Chehbouni, A. A process-based modelling of groundwater recharge under contrasting irrigation methods in semi-arid crops. *Agric. Water Manag.* **2025**, *316*, 109584. [CrossRef]
10. Modanesi, S.; Massari, C.; Bechtold, M.; Lievens, H.; Tarpanelli, A.; Brocca, L.; Zappa, L.; De Lannoy, G.J.M. Challenges and benefits of quantifying irrigation through the assimilation of Sentinel-1 backscatter observations into Noah-MP. *Hydrol. Earth Syst. Sci.* **2022**, *26*, 4685–4706. [CrossRef]
11. Ait Brahim, Y.; Bouchaou, L.; Sifeddine, A.; Khodri, M.; Reichert, B.; Cruz, F.W. Elucidating the climate and topographic controls on stable isotope composition of meteoric waters in Morocco, using station-based and spatially-interpolated data. *J. Hydrol.* **2016**, *543*, 305–315. [CrossRef]

12. Liu, Y.; Zhu, G.; Zhang, Z.; Sun, Z.; Yong, L.; Sang, L.; Wang, L.; Zhao, K. Isotopic differences in soil–plant–atmosphere continuum composition and control factors of different vegetation zones on the northern slope of the Qilian Mountains. *Biogeosciences* **2022**, *19*, 877–889. [CrossRef]
13. Tetzlaff, D.; Buttle, J.; Carey, S.K.; Kohn, M.J.; Laudon, H.; McNamara, J.P.; Smith, A.; Sprenger, M.; Soulsby, C. Stable isotopes of water reveal differences in plant—Soil water relationships across northern environments. *Hydrol. Process.* **2021**, *35*, e14023. [CrossRef]
14. Ceperley, N.; Gimeno, T.E.; Jacobs, S.R.; Beyer, M.; Dubbert, M.; Fischer, B.; Geris, J.; Holko, L.; Kübert, A.; le Gall, S.; et al. Toward a common methodological framework for the sampling, extraction, and isotopic analysis of water in the Critical Zone to study vegetation water use. *WIREs Water* **2024**, *11*, e1727. [CrossRef]
15. Aouade, G.; Ezzahar, J.; Amenzou, N.; Er-Raki, S.; Benkaddour, A.; Khabba, S.; Jarlan, L. Combining stable isotopes, Eddy Covariance system and meteorological measurements for partitioning evapotranspiration, of winter wheat, into soil evaporation and plant transpiration in a semi-arid region. *Agric. Water Manag.* **2016**, *177*, 181–192. [CrossRef]
16. Orlowski, N.; Breuer, L.; Angeli, N.; Boeckx, P.; Brumbt, C.; Cook, C.S.; Dubbert, M.; Dyckmans, J.; Gallagher, B.; Gralher, B.; et al. Inter-laboratory comparison of cryogenic water extraction systems for stable isotope analysis of soil water. *Hydrol. Earth Syst. Sci.* **2018**, *22*, 3619–3637. [CrossRef]
17. Wang, X.-F.; Yakir, D. Using stable isotopes of water in evapotranspiration studies. *Hydrol. Process.* **2000**, *14*, 1407–1421. [CrossRef]
18. Helliker, B.R.; Ehleringer, J.R. Differential 18O enrichment of leaf cellulose in C3 versus C4 grasses. *Funct. Plant Biol.* **2002**, *29*, 435–442. [CrossRef] [PubMed]
19. Williams, D.G.; Cable, W.; Hultine, K.; Hoedjes, J.C.B.; Yepez, E.A.; Simonneaux, V.; Er-Raki, S.; Boulet, G.; de Bruin, H.A.R.; Chehbouni, A.; et al. Evapotranspiration components determined by stable isotope, sap flow and eddy covariance techniques. *Agric. For. Meteorol.* **2004**, *125*, 241–258. [CrossRef]
20. Ehleringer, J.R.; Dawson, T.E. Water uptake by plants: Perspectives from stable isotope composition. *Plant Cell Environ.* **1992**, *15*, 1073–1082. [CrossRef]
21. Kuppel, S.; Tetzlaff, D.; Maneta, M.P.; Soulsby, C. EcH2O-iso 1.0: Water isotopes and age tracking in a process-based, distributed ecohydrological model. *Geosci. Model Dev.* **2018**, *11*, 3045–3069. [CrossRef]
22. Murad, A.; Krishnamurthy, R.V. Factors controlling the stable hydrogen and carbon isotoperatios in regional ground water of the Eastern United Arab Emirates (UAE). *Hydrol. Process.* **2007**, *22*, 1922–1931. [CrossRef]
23. Mohammed, A.M.; Krishnamurthy, R.V.; Kehew, A.E.; Crossey, L.J.; Karlstrom, K.K. Factors affecting the stable isotopes ratios in groundwater impacted by intense agricultural practices: A case study from the Nile Valley of Egypt. *Sci. Total Environ.* **2016**, *573*, 707–715. [CrossRef] [PubMed]
24. Craig, H.; Gordon, L.I.; Horibe, Y. Isotopic exchange effects in the evaporation of water: 1. Low-temperature experimental results. *J. Geophys. Res.* **1963**, *68*, 5079–5087. [CrossRef]
25. le Page, M.; Toumi, J.; Khabba, S.; Hagolle, O.; Tavernier, A.; Kharrou, M.; Er-Raki, S.; Huc, M.; Kasbani, M.; Moutamanni, A.; et al. A Life-Size and Near Real-Time Test of Irrigation Scheduling with a Sentinel-2 Like Time Series (SPOT4-Take5) in Morocco. *Remote Sens.* **2014**, *6*, 11182–11203. [CrossRef]
26. Nassah, H.; Younes, F.; Salah, E.; Said, K.; Mougenot, B. Mapping Soil Clay Content and Hydraulic Properties over an Agricultural Semiarid Plain Using Remote Sensing and Interpolation Techniques. *Ecol. Eng. Environ. Technol.* **2024**, *25*, 164–179. [CrossRef]
27. Wösten, J.H.M. Chapter 10 Pedotransfer functions to evaluate soil quality. *Dev. Soil Sci.* **1997**, *25*, 221–245. [CrossRef]
28. Zhou, L.; Zhang, Z.; Zhang, W.; An, K.; Lei, X.; He, M. Real-Time Water Level Prediction in Open Channel Water Transfer Projects Based on Time Series Similarity. *Water* **2022**, *14*, 2070. [CrossRef]
29. Williams, M.R.; Lartey, J.L.; Sanders, L.L. Isotopic (δ^{18}O and δ^{2}H) Integrity of Water Samples Collected and Stored by Automatic Samplers. *Agric. Environ. Lett.* **2018**, *3*, 180009. [CrossRef]
30. Tsuruta, K.; Yamamoto, H.; Katsuyama, M.; Kosugi, Y.; Okumura, M.; Matsuo, N. Effects of cryogenic vacuum distillation on the stable isotope ratios of soil water. *Hydrol. Res. Lett.* **2019**, *13*, 1–6. [CrossRef]
31. Wang, D.; Risi, C.; Tian, L.; Yang, D.; Bowen, G.; Fan, S.; Su, Y.; Pang, H.; Li, L. Correcting for water vapor diffusion in air bag samples for isotope composition analysis: Cases studies with drone-collected samples. *Preprints* **2024**. [CrossRef]
32. Boukhari, K.; Fakir, Y.; Stigter, T.Y.; Hajhouji, Y.; Boulet, G. Origin of recharge and salinity and their role on management issues of a large alluvial aquifer system in the semi-arid Haouz plain, Morocco. *Environ. Earth Sci.* **2015**, *73*, 6195–6212. [CrossRef]
33. Yang, Y.; Zhang, M.; Wang, S.; Qu, D.; Zhang, Y.; Wang, J. Soil moisture variability affected by sand mulch: An isotope-based assessment of irrigated farmland in Northwest China. *Ecohydrology* **2023**, *16*, 2477. [CrossRef]
34. Oshun, J.; Dietrich, W.E.; Dawson, T.E.; Fung, I. Dynamic, structured heterogeneity of water isotopes inside hillslopes. *Water Resour. Res.* **2016**, *52*, 164–189. [CrossRef]
35. Singleton, M.J.; Sonnenthal, E.L.; Conrad, M.E.; DePaolo, D.J.; Gee, G.W. Multiphase Reactive Transport Modeling of Seasonal Infiltration Events and Stable Isotope Fractionation in Unsaturated Zone Pore Water and Vapor at the Hanford Site. *Vadose Zone J.* **2004**, *3*, 775–785. [CrossRef]

36. Sprenger, M.; Leistert, H.; Gimbel, K.; Weiler, M. Illuminating hydrological processes at the soil-vegetation-atmosphere interface with water stable isotopes. *Rev. Geophys.* **2016**, *54*, 674–704. [CrossRef]
37. Orlowski, N.; Seeger, S.; Mennekes, D.; de Boer, H.; Weiler, M.; Rinderer, M. Monitoring tree species-specific water uptake strategies via continuous in-situ stable water isotope measurements. In Proceedings of the EGU General Assembly, Online, 4–8 May 2020; EGU2020-16786. [CrossRef]
38. Barbeta, A.; Gimeno, T.E.; Clavé, L.; Fréjaville, B.; Jones, S.P.; Delvigne, C.; Wingate, L.; Ogée, J. An explanation for the isotopic offset between soil and stem water in a temperate tree species. *New Phytol.* **2020**, *227*, 766–779. [CrossRef] [PubMed]
39. Amin, A.; Zuecco, G.; Marchina, C.; Engel, M.; Penna, D.; McDonnell, J.J.; Borga, M. No evidence of isotopic fractionation in olive trees (*Olea europaea*): A stable isotope tracing experiment. *Hydrol. Sci. J.* **2021**, *66*, 2415–2430. [CrossRef]
40. Dansgaard, W. Stable isotopes in precipitation. *Tellus A Dyn. Meteorol. Oceanogr.* **2012**, *16*, 436. [CrossRef]
41. Nasta, P.; Todini-Zicavo, D.; Zuecco, G.; Marchina, C.; Penna, D.; McDonnell, J.J.; Amin, A.; Allocca, C.; Marzaioli, F.; Stellato, L.; et al. Quantifying irrigation uptake in olive trees: A proof-of-concept approach combining isotope tracing and Hydrus-1D. *Hydrol. Sci. J.* **2023**, *68*, 1479–1486. [CrossRef]
42. Brighenti, S.; Tagliavini, M.; Comiti, F.; Aguzzoni, A.; Giuliani, N.; Abdelkader, A.B.; Penna, D.; Zanotelli, D. Drip irrigation frequency leads to plasticity in root water uptake by apple trees. *Agric. Water Manag.* **2024**, *298*, 108870. [CrossRef]
43. Penna, D.; Geris, J.; Hopp, L.; Scandellari, F. Water sources for root water uptake: Using stable isotopes of hydro--gen and oxygen as a research tool in agricultural and agroforestry systems. *Agric. Ecosyst. Environ.* **2020**, *291*, 106790. [CrossRef]
44. Sprenger, M.; Allen, S.T. Commentary: What ecohydrologic separation is and where we can go with it. *Water Resour. Res.* **2020**, *56*, e2020WR027238. [CrossRef]
45. Beyer, M.; Kühnhammer, K.; Dubbert, M. In situ measurements of soil and plant water isotopes: A review of approaches, practical considerations and a vision for the future. *Hydrol. Earth Syst. Sci.* **2020**, *24*, 4413–4440. [CrossRef]
46. Zhang, X.; Wang, Y.; Li, P.; Zhou, X. Improving sampling protocols for stable isotope analysis in agro-ecosystems. *J. Hydrol.* **2023**, *617*, 129031. [CrossRef]
47. Koeniger, P.; Gaj, M.; Wassenaar, L.I. Evaporation-induced oxygen-18 and deuterium enrichment in water sample storage: Field guidance for precipitation collectors. *Hydrol. Process.* **2020**, *34*, 921–925.
48. Oerter, E.J.; Siebert, G.; Bowling, D.R.; Bowen, G. Soil water vapour isotopes identify missing water source for streamside trees. *Ecohydrology* **2019**, *12*. [CrossRef]
49. Johansen, T.; Crispin, M.; White, S. Advances in cryogenic vacuum distillation for stable isotope analysis. *Anal. Methods* **2021**, *14*, 1090–1102.
50. Mahindawansha, A.; Orlowski, N.; Kraft, P.; Rothfuss, Y.; Racela, H.; Breuer, L. Quantification of plant water uptake by water stable isotopes in rice paddy systems. *Plant Soil* **2018**, *429*, 281–302. [CrossRef]
51. Zhao, L.; Zhang, J.; Liu, H.; Yang, M. Using stable isotopes to trace soil water movement in a semi-arid watershed. *Hydrol. Process.* **2020**, *34*, 103–116. [CrossRef]
52. Rothfuss, Y.; Javaux, M. Reviews and syntheses: Isotopic approaches to quantify root water uptake: A review and comparison of methods. *Biogeosciences* **2017**, *14*, 2199–2224. [CrossRef]

Disclaimer/Publisher's Note: The statements, opinions and data contained in all publications are solely those of the individual author(s) and contributor(s) and not of MDPI and/or the editor(s). MDPI and/or the editor(s) disclaim responsibility for any injury to people or property resulting from any ideas, methods, instructions or products referred to in the content.